

Original Article

Molecular tumor targeting of gelonin by fusion with F3 peptide

Song-Hee HAM^{1, #}, Kyoung Ah MIN^{2, #}, Meong Cheol SHIN^{1, *}

¹College of Pharmacy and Research Institute of Pharmaceutical Sciences, Gyeongsang National University, Jinju, Gyeongnam 660–701, Republic of Korea; ²College of Pharmacy, Inje University, Gimhae, Gyeongnam 621–749, Republic of Korea

Abstract

Therapeutically potent macromolecular drugs have shown great promise for overcoming the limitations of small-molecule anti-cancer drugs. But tumor cell-selective intracellular delivery of the macromolecules remains a major hurdle for their successful clinical application. To overcome this challenge, we engineered a novel genetic fusion protein (F3-Gel) that composed of F3 peptide, a tumor-homing peptide, and gelonin, a plant-derived ribosome-inactivating protein (RIP), and then evaluated its anti-cancer activity *in vitro* and *in vivo*. The F3-Gel-encoding gene was synthesized by genetic recombination, and F3-Gel was successfully expressed in *E. coli*. The anti-cancer activity of the produced F3-Gel was evaluated by various *in vitro* assays, which revealed that F3-Gel maintained equipotent protein synthesis inhibition activity (IC₅₀=11 pmol/L) as unmodified gelonin (IC₅₀=10 pmol/L). Furthermore, F3-Gel displayed enhanced cellular uptake into cancer cells (U87 MG, HeLa, LnCaP and 9L) than noncancerous cells (293 HEK and SVGp12). Compared with gelonin, F3-Gel exerted significantly higher cytotoxicity against these cancer cells. F3-Gel displayed significantly greater inhibition of protein translation in U87 MG cells: F3-Gel (0.5 μmol/L) was able to reduce the protein level to less than 50%, while gelonin (1 μmol/L) did not affect the intracellular protein level. In a U87 MG xenograft tumor-bearing mouse model, F3-Gel was accumulated in the tumor site at much higher levels and maintained for a prolonged time compared with gelonin. Administration of F3-Gel (0.5, 0.75 mol/kg, iv) caused 36% and 66%, respectively, inhibition of tumor growth in U87 MG xenograft mice, suggesting that it is a promising candidate drug for cancer treatment. Furthermore, this study demonstrates that fusion of F3 peptide to a potent macromolecule could provides an effective method for targeting tumors and eventually could improve their druggability.

Keywords: gelonin; toxin; F3 peptide; selective tumor targeting; glioblastoma

Acta Pharmacologica Sinica (2017) 38: 897–906; doi: 10.1038/aps.2017.20; published online 17 Apr 2017

Introduction

Cancer chemotherapeutics have primarily depended on the use of small molecular agents that possess little selectivity for cancer cells. While some have been efficacious in eradicating tumor cells, most of these small molecular drugs have led to severe toxicities against normal tissues^[1–3]. Those side effects can prevent the administration of effective drug doses that are sufficient to kill cancer cells. Various molecular markers, selectively expressed on tumor cell surfaces, that distinguish tumor cells from normal cells provide the basis for the design of targeted, molecular-based cancer therapies. To date, various approaches based on ligand-targeted therapeutics (*ie*, antibodies, tumor-homing peptides or small molecular

ligands) that can specifically bind to tumor-associated markers (*ie*, receptors) have been utilized to selectively kill tumor cells^[4–6]. As an active targeting tool, antibodies bound to the cell surface antigens can promote the induction of antitumor immune responses by manipulating tumor-related signaling^[7] or concentrate conjugated drug molecules to tumor cells expressing specific antigens^[8, 9]. However, there are risks that antibody-based therapeutics might cause other problematic immune responses such as anti-idiotypic responses against humanized or fully human antibodies^[10, 11]. Critically, tumor penetration by antibodies is known to be quite poor due to their large size (150 kDa) and high binding affinity to antigens, with the latter being termed the binding-site barrier^[4, 12]. Diffusion of high-affinity antibodies into tumors can be limited because the slow rates of dissociation decrease the local concentration of diffusible, free antibody.

Meanwhile, peptide ligands have been drawing enormous interest because of their crucial merits over conventional

These authors contributed equally to this work.

*To whom correspondence should be addressed.

E-mail shinmc@gnu.ac.kr

Received 2016-11-20 Accepted 2017-01-20

ligands (eg, antibodies) mainly owing to their relatively small size^[4, 13]. Peptide ligands with smaller sizes can provide 1) a decreased possibility of affecting the function of the coupled drug, especially enzyme drugs, 2) availability of multivalency and 3) less immunogenicity^[14, 15]. Various peptide ligands have recently been developed due to the advancement of technologies for discovering novel peptides that can selectively bind to tumor cells, such as phage-display cDNA libraries. One of these recently discovered peptides that has garnered much interest is the F3 peptide^[16, 17]. F3 is a 30–34-amino acid fragment of a high mobility group protein, HMG2N. Nucleolin is known to be highly expressed on the surface of tumor cells, whereas it is primarily expressed in the cytoplasm and nuclear membrane in normal cells, which might help to achieve selective drug targeting into the tumor site^[18]. These receptor molecules expressed on the tumor cell surface are known to play an important role in facilitating the internalization of F3 peptide into tumor cells and transport into the cell nucleus. F3 peptide can bind to tumor cells expressing nucleolins or endothelial cells as angiogenesis precursors^[19]. Therefore, macromolecular drugs conjugated with F3 peptides might be efficiently internalized into tumor cells via nucleolin-mediated transport, resulting in enhanced cancer therapeutic effects.

With unmatched potency and selectivity, macromolecular drugs (ie, proteins or genes) have drawn interest over the past few decades for overcoming the limitations of small molecular drugs, which are accompanied by side effects and toxicity at therapeutic dosages^[20–22]. Gelonin, a plant-derived protein toxin, is one of the macromolecular drug candidates. It is a 30 kDa glycoprotein that was first derived from the seeds of *Gelonium multiflorum*. As a ribosome-inactivating protein (RIP) toxin, gelonin inhibits protein synthesis via the cleavage of a single adenine residue (A₄₃₂₄) in the 28S ribosomal RNA^[23]. The potency of gelonin in inhibiting protein translation is so high that even a single gelonin molecule can kill one tumor cell after cellular uptake^[23]. However, despite the high potency of gelonin, its clinical translation as an anti-cancer drug remains a challenge because of its poor cellular uptake. To overcome this challenge of intracellular delivery, we previously synthesized various gelonin fusion proteins with different membrane-active peptides (eg, low molecular weight protamine, TAT peptide and melittin) and tested the constructs in different tumor cell lines^[24–26]. Despite achieving significantly improved cellular uptake, these fusion proteins lacked cell selectivity for their activity, and the toxicity concern remained a great obstacle for clinical application of these fusion proteins. In this regard, in this study, we developed an F3-gelonin (F3-Gel) fusion chimera through recombinant technologies. The inhibitory activity of this recombinant protein on protein synthesis in tumor cells was assessed using a cell-free translational system (ie, a rabbit reticulocyte lysate assay). Furthermore, the potency against tumor cells was examined in various cancer cell lines and *in vivo* with animal experiments using a U87 MG xenograft tumor-bearing mouse model.

Materials and methods

Materials

DNA restriction enzymes (*Nde* I and *Nhe* I) and T4 DNA ligase were purchased from New England Biolabs (Ipswich, MA, USA). Competent *E coli* strains [TOP10 and BL21star (DE3)] were purchased from Invitrogen (Carlsbad, CA, USA). Isopropyl β -D-1-thiogalactopyranoside (IPTG) and carbenicillin were purchased from Fisher Scientific (Pittsburg, PA, USA). AcTEVTM protease, PBS (pH 7.4), Dulbecco's modified Eagle's medium (DMEM), fetal bovine serum albumin (FBS) and Hoechst 33342 were purchased from Invitrogen (Carlsbad, CA, USA). A BCA assay kit was purchased from Bio-Rad Laboratories (Hercules, CA, USA). The rabbit reticulocyte lysate assay system was purchased from Promega Corporation (Madison, WI, USA). Rhodamine B isothiocyanate (TRITC) was purchased from Sigma-Aldrich (St Louis, MO, USA). A cell proliferation kit II (XTT) was purchased from Roche Applied Science (Indianapolis, IN, USA), and DylightTM 775-B4 was purchased from Thermo Fisher Scientific (Rockford, IL, USA).

Expression of F3-gelonin fusion protein

The schematic design of the pET-TRX-F3-Gel vector for the expression of the F3 peptide-fused gelonin is shown in Figure 1A and 1B. Genes encoding a portion of the N-terminal region of gelonin and an F3 peptide (299 bp; GenScript USA Inc, Piscataway, NJ, USA) were double digested (*Nde* I and *Nhe* I) from a pUC-57 simple vector, and the gene fragments were separated on a 1% agarose gel, purified, and ligated into a linearized pET22b-TRX-Gel vector previously prepared in our lab^[24]. The constructed pET-TRX-F3-Gel was submitted for DNA sequencing analysis.

A single colony of BL21 (DE3) transformed with pET-TRX-F3-Gel grown on LB agar plates containing 50 μ g/mL of carbenicillin, was picked and used to inoculate 40 mL of LB broth (50 μ g/mL of carbenicillin). The starter culture was incubated overnight at 37°C with shaking at 250 rounds per minute and then diluted into 1 L of LB broth. The large (1 L) culture was incubated under the same conditions until the absorbance at OD₆₀₀ reached 1.0. IPTG was added as an inducer to a final concentration of 0.5 mmol/L, and the cultures were further incubated for 4 h. After incubation, cells were harvested by centrifugation, re-suspended in 20 mmol/L PBS (300 mmol/L NaCl, pH 7) and then lysed by sonication (4 \times 30 s, with 50% output in ice bath). After centrifugation, the supernatant fractions were loaded onto HisPure[®] Ni-NTA resin (Bio-Rad Laboratories, Hercules, CA, USA), and after being washed with PBS, thioredoxin-6 \times His tagged F3-gelonin (TRX-F3-Gel) was eluted with 300 mmol/L imidazole (20 mmol/L PBS, 300 mmol/L NaCl, 300 mmol/L imidazole, pH 7). To remove the thioredoxin-6 \times His tag, TRX-F3-Gel was incubated with TEV protease (AcTEVTM protease, Invitrogen), and F3-Gel was purified with a heparin column using a salt gradient (0 to 2 mol/L NaCl at a rate of 0.02 mol \cdot L⁻¹ \cdot min⁻¹, flow rate: 1 mL/min). Recombinant gelonin was expressed using a pET28a-Gel vector and purified following the identical procedures described

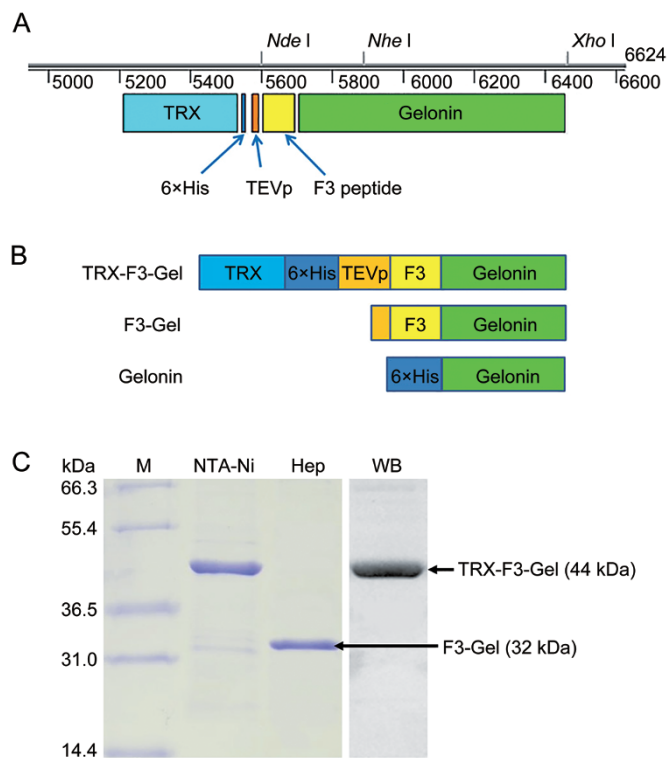


Figure 1. Schematic design of F3-Gel and proof of production. (A) Schematic design of pET-F3-Gel vector. The pET-F3-Gel vector was constructed by inserting the N-terminal sequence of gelonin and F3-gelonin gene into a pET-TRX vector containing the thioredoxin (TRX) gene. (B) Schematic images of TRX-F3-Gel, F3-Gel and Gelonin. (C) SDS-PAGE results of Ni-NTA and heparin column purification of TRX-F3-Gel. Lane M: markers of the protein molecular weight standard (Mark 12™ standard, Invitrogen). Lane NTA-Ni: TRX-F3-Gel purified by a Ni-NTA column. Lane Hep: fraction obtained by heparin column purification of F3-Gel after cleavage of thioredoxin-6×His tag from the TRX-F3-Gel. Lane WB: Western blot assay results of TRX-F3-Gel. The purity of the final F3-Gel product was determined based on densitometry analysis using ImageJ software. TRX-F3-Gel: recombinant thioredoxin-6×His tagged-F3-gelonin fusion protein; F3-Gel: recombinant F3-gelonin fusion protein, Gelonin: recombinant gelonin.

by Shin *et al*^[24].

Protein assays

The expression of soluble TRX-F3-Gel was determined by SDS-PAGE and Western blot analysis, and every purification step was monitored by SDS-PAGE on a 10% Tris-HCl gel. For the Western blot assay, resolved protein bands were transferred to a nitrocellulose membrane, and after blocking, the membrane was washed with TBS-T buffer (50 mmol/L Tris, 0.15 mol/L NaCl, 0.1% Tween 20) and incubated with a primary antibody (mouse anti-6×His tag Ab, Abcam) at 4°C overnight. Then, the membranes were washed again with TBS-T buffer and incubated with a secondary antibody (alkaline phosphatase (AP)-conjugated anti-mouse IgG, Sigma-Aldrich) for 1 h at room temperature. After incubation, the membrane was washed with TBS-T buffer, and protein bands were developed

with Nitroblue tetrazolium chloride/5-bromo-4-chloro-3'-indolylphosphate p-toluidine salt substrate (NBT/BCIP, Roche) in a buffer containing 0.1 mol/L Tris-HCl, 0.1 mol/L NaCl, and 0.05 mol/L MgCl₂ at pH 9.5. The purity of the final F3-Gel product was determined based on densitometry analysis using ImageJ software (National Institutes of Health, Bethesda, MD, USA), and the production yield was calculated using a BCA protein assay.

Protein synthesis inhibition assay

Protein translation inhibition by F3-Gel was assessed, in comparison with gelonin, using a rabbit reticulocyte lysate assay following the procedures of Shin *et al*^[24].

Cell culture

U87 MG human glioblastoma-astrocytoma, 9L rat glioma, HeLa, LnCaP, 293 HEK (human embryonic kidney) and SVGP12 cell lines were purchased from American Type Culture Collection (ATCC, Manassas, VA, USA). Cell cultures were maintained in complete medium (DMEM with 10% FBS and 1% penicillin-streptomycin antibiotics).

Cellular uptake

HeLa, LnCaP, 9L, U87 MG, 293 HEK and SVGP12 cells were seeded onto 24-well plates at 5×10^4 cells per well and incubated in complete medium. After 24 h of incubation, TRITC-labeled F3-Gel and gelonin were added to the wells and incubated at 37°C for 4 h in a humidified CO₂ incubator. To evaluate whether the entry of F3-Gel is F3-specific, a separate group of U87 MG cells were pre-treated with unlabeled free F3 peptides (5-fold to the F3-Gel) for 30 min and then incubated with the TRITC-labeled F3-Gel for 4 h. After incubation, the cells were washed three times with PBS, and nuclei were counterstained with Hoechst 33342. Following the Hoechst staining, the cells were washed with PBS again, and images of the live cells were acquired using a Nikon A1R-A1 confocal microscope. Cell images were analyzed with NIS-elements software (Nikon Instruments Inc, Melville, NY, USA).

For quantitative analysis of the cellular uptake, cells seeded on 24-well plates were incubated with either TRITC-labeled gelonin or F3-Gel up to 4 h. Then, at certain time points (0, 0.5, 1, 2 and 4 h post-incubation), the cells were lysed and the fluorescence intensities of the lysates were measured.

Cytotoxicity assay

HeLa, LnCaP, 9L, U87 MG, 293 HEK and SVGP12 cells were dispensed into 96-well plates at a density of 5×10^3 cells per well and incubated in a humidified CO₂ incubator. After 24 h of incubation, F3-Gel and gelonin were separately added to the wells at varying final concentrations (10^{-11} - 10^{-5} mol/L), and the cells were further incubated for 48 h. Then, the relative cell viability was determined using an XTT assay following the manufacturer's instructions (Roche Applied Science, Indianapolis, IN, USA). The IC₅₀ values of the F3-Gel and gelonin were calculated using Prism software (Prism version 5.0, GraphPad, CA, USA).

Intracellular activity of F3-Gel for inhibition of protein translation

U87 MG cells were seeded onto 12-well plates (10^5 cells per well) and incubated overnight. Cells were then treated with either 1) PBS, 2) gelonin or 3) F3-Gel at final concentrations of 0.1, 0.5 or 1 $\mu\text{mol/L}$. After 24 h of incubation, cells were washed with PBS and then lysed by incubation with 1% Triton-X 100. After centrifugation, the protein in the supernatant was quantified using a BCA protein assay. Relative cellular protein levels (%) were calculated by dividing the protein amount in the sample-treated cells by that of the PBS-treated control cells.

Tissue distribution of F3-Gel

Male athymic nude mice (body weight: 22–26 g) were purchased from Charles Rivers Laboratories (Raleigh, NC, USA). Three days after arrival, U87 MG cells (10^7 cells per mouse) were implanted (sc) in the left flank of the mice, and when the average size of the tumor reached 500 mm^3 , either gelonin or F3-Gel labeled with near-infrared dye (DylightTM 775-B4, Thermo Scientific, Rockford, IL, USA) was injected (0.25 $\mu\text{mol/kg}$) into the mice via the tail vein. Then, at certain time points (1, 4 and 16 h post-administration), mice were euthanized, and their major organs (eg, tumor, heart, liver, spleen, lung, kidney and intestine) were harvested. The fluorescence intensities of these organs were measured with an IVIS[®] spectrum imaging system (Xenogen, Alameda, CA, USA). Images of the organs were collected using an ICG filter (Ex/Em: 745 nm/800 nm) with identical illumination settings, and the images were analyzed with Living Image 2.5 software (Xenogen, Alameda, CA, USA). The mean fluorescence intensities of the organs were normalized by the weights of organs.

Tumor growth inhibition by F3-Gel

U87 MG sc xenograft tumor-bearing mice were randomly divided into 6 groups when the tumor size reached an average of 200 mm^3 (d 11 after tumor implantation) and administered either 1) PBS, 2) gelonin (0.75 $\mu\text{mol/kg}$), 3) F3-Gel (0.125 $\mu\text{mol/kg}$), 4) F3-Gel (0.25 $\mu\text{mol/kg}$), 5) F3-Gel (0.5 $\mu\text{mol/kg}$) or 6) F3-Gel (0.75 $\mu\text{mol/kg}$). The mice were treated a total of three times with one of the above recipes at d 11, 14 and 17 via tail vein injection. Every day, the tumor volume and body weight of the mice were measured until the average tumor size of the PBS control group reached 1000 mm^3 .

Statistical analysis

Plots were generated with error bars (SEM) using GraphPad Prism 5.0 (San Diego, CA, USA). Data analyses between two groups were performed with a two-tailed unpaired Student's *t*-test. Statistical analyses among groups were conducted by one-way analysis of variance (ANOVA), followed by a *post hoc* Tukey's multiple comparison test as needed. The results that yielded $P < 0.05$ were considered statistically significant.

Results

Expression and purification of F3-gelonin fusion protein (F3-Gel)

F3-Gel was expressed as a soluble and functional protein from

E. coli. As shown in Figure 1C, expression of thioredoxin-6 \times His tagged-F3-gelonin (a.k.a. TRX-F3-Gel) and successful cleavage of the TRX after incubation with TEV protease were confirmed from the SDS-PAGE and Western blot assay results. The final yield of the F3-Gel product was an average of 2 mg per liter of culture, and the purity was above 90%, determined by densitometry analysis of the resolved gel image using ImageJ software (National Institutes of Health, Bethesda, MD, USA).

Protein synthesis inhibition by F3-Gel

As shown in Figure 2, both F3-Gel and unmodified gelonin showed similar inhibitory activity against cell-free translation of luciferase, indicating that fusion of the F3 peptide and gelonin did not affect the intrinsic catalytic activity of gelonin. The concentrations for 50% inhibition (IC_{50}) of protein translation by gelonin (10 pmol/L) and F3-Gel (11 pmol/L) were not statistically different.

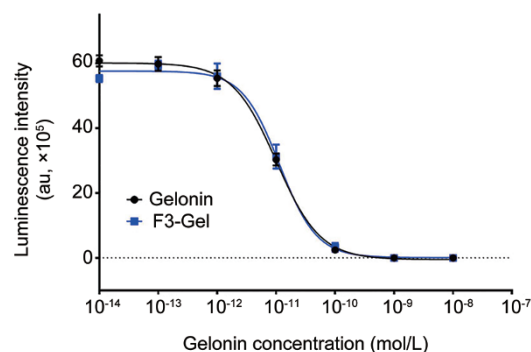


Figure 2. Protein synthesis inhibition by F3-Gel. Inhibition of protein translation by unmodified gelonin (Gelonin) and recombinant F3-gelonin fusion protein (F3-Gel) was determined using a cell-free translational system and luciferase as the marker. The quantity of the translated luciferase was measured using a chemiluminescent assay (mean \pm SEM; $n=3$). Luminescence intensity vs gelonin concentration curves were fitted by a nonlinear regression model using Prism software.

Selective uptake by tumor cells

A cellular uptake study was performed to examine whether F3 can induce selective uptake of F3-Gel into various cancer (HeLa, LnCaP, 9L and U87 MG) over noncancerous (293 HEK and SVGP12) cells. Representative confocal microscopy images of live 293 HEK and U87 MG cells, acquired after incubation with TRITC-labeled gelonin or F3-Gel, are displayed in Figure 3A. As seen, the fluorescence signal was barely visible in 293 HEK cells incubated with either gelonin or F3-Gel or in gelonin-treated U87 MG cells, while the fluorescence intensity was clearly observed in the F3-Gel-treated U87 MG cells. However, with pretreatment of excessive F3 peptide, the fluorescence signal from U87 MG cells was severely reduced. Quantitative analyses of the cellular uptake results for U87 MG and 293 HEK cells (Figure 3B) were consistent with the observations from the confocal microscopy images. After

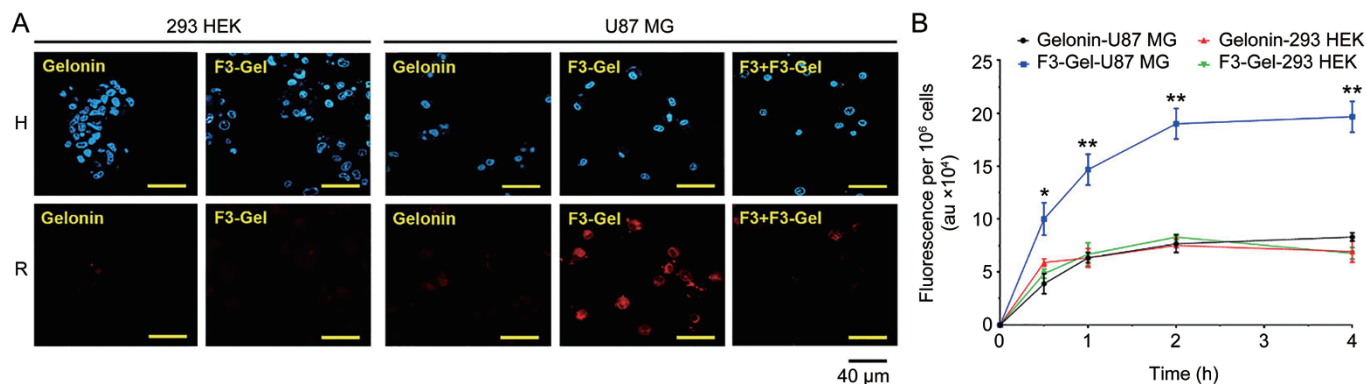


Figure 3. Cell uptake study results of gelonin and F3-Gel on 293 HEK noncancerous cells and U87 MG cancer cells. (A) Confocal microscopy images of live cells after incubation with either TRITC-labeled gelonin or F3-Gel for 4 h at 37 °C. After incubation, the cells were washed three times with PBS, the nuclei were counterstained with Hoechst 33342, and after being washed with PBS, the cell images were acquired with a confocal microscope utilizing Hoechst (H; blue) and rhodamine (R; red) channels. Scale bar indicates 40 μm. (B) Quantitative analysis of cellular uptake of gelonin or F3-Gel in U87 MG and 293 HEK cells (mean±SEM. *n*=3. **P*<0.05, ***P*<0.01 by *t*-tests). Fluorescence intensity values per 10⁶ cells are depicted over the incubation time period (until 4 h).

4 h of incubation, the fluorescence intensity of U87 MG cells incubated with F3-Gel was 1.4-fold greater than that of F3-Gel-treated 293 HEK cells, while there was no difference in the cellular uptake of gelonin. Only the F3-Gel-treated U87 MG cells exhibited statistically significant differences in fluorescence intensity among the 4 groups. As shown in Table 1, when the cell internalization profiles of gelonin and F3-Gel were compared for 6 different cell lines, including cancer and noncancerous cells, a significantly higher uptake of F3-Gel was observed in all the tested cancer cells but not in the noncancerous cells.

Anti-cancer activity

Cell viability studies were performed with various cancer (eg, HeLa, LnCaP, 9L, U87 MG) and noncancerous (293 HEK and SVGp12) cell lines via an XTT assay. The cell viability-versus-gelonin concentration profiles are shown in Figure 4, and the calculated IC₅₀ values are summarized in Table 2. As seen, only mild cytotoxicity was observed in gelonin-treated cells (avg. IC₅₀: 2.0–2.9 μmol/L), possibly due to cell internalization via fluid phase pinocytosis. In sharp contrast, significantly higher cytotoxicity (avg. IC₅₀: 0.33–0.41 μmol/L) was observed in the cancer cell lines (HeLa, LnCaP, 9L and U87 MG) incu-

Table 1. Fluorescence intensity values (×10⁴) related with the intracellular level of gelonin and F3-Gel into various cancer and noncancerous cell lines.

Samples	HeLa	LnCaP	9L	U87 MG	293 HEK	SVGp12
Gelonin ^a	7.2±0.5	5.7±0.7	6.4±0.9	7.7±1.5	7.5±1.1	6.8±0.8
F3-Gel ^a	14.3±3.3*	12.7±0.7**	21.9±2.3**	20.4±5.8*	8.6±0.9*	8.0±0.8*
Fold difference ^b	2.0	2.2	3.4	2.7	1.1	1.2

^a Fluorescence intensity measurements per 10⁶ cells (×10⁴) after 4 h incubation with TRITC-labeled gelonin or F3-Gel are displayed for each cell-type.

P*<0.05, *P*<0.01. For all experiments, *n*=3. F3-Gel: recombinant F3-gelonin chimera.

^b Fold difference is calculated from dividing fluorescence intensity values from F3-Gel-treated cells by those from gelonin-treated cells for each cell-type.

Table 2. Cytotoxicity levels (IC₅₀) of gelonin and F3-Gel.

Samples	HeLa	LnCaP	9L	U87 MG	293 HEK	SVGp12
Gelonin ^a	2.00±0.50	2.70±0.72	2.50±0.51	2.10±0.85	2.80±0.53	2.90±0.75
F3-Gel ^a	0.34±0.11**	0.41±0.12**	0.39±0.05**	0.33±0.08**	2.30±0.38	2.80±0.25

^a IC₅₀ values are displayed as μmol/L. ***P*<0.01. For all experiments, *n*=3. F3-Gel: recombinant F3-gelonin chimera.

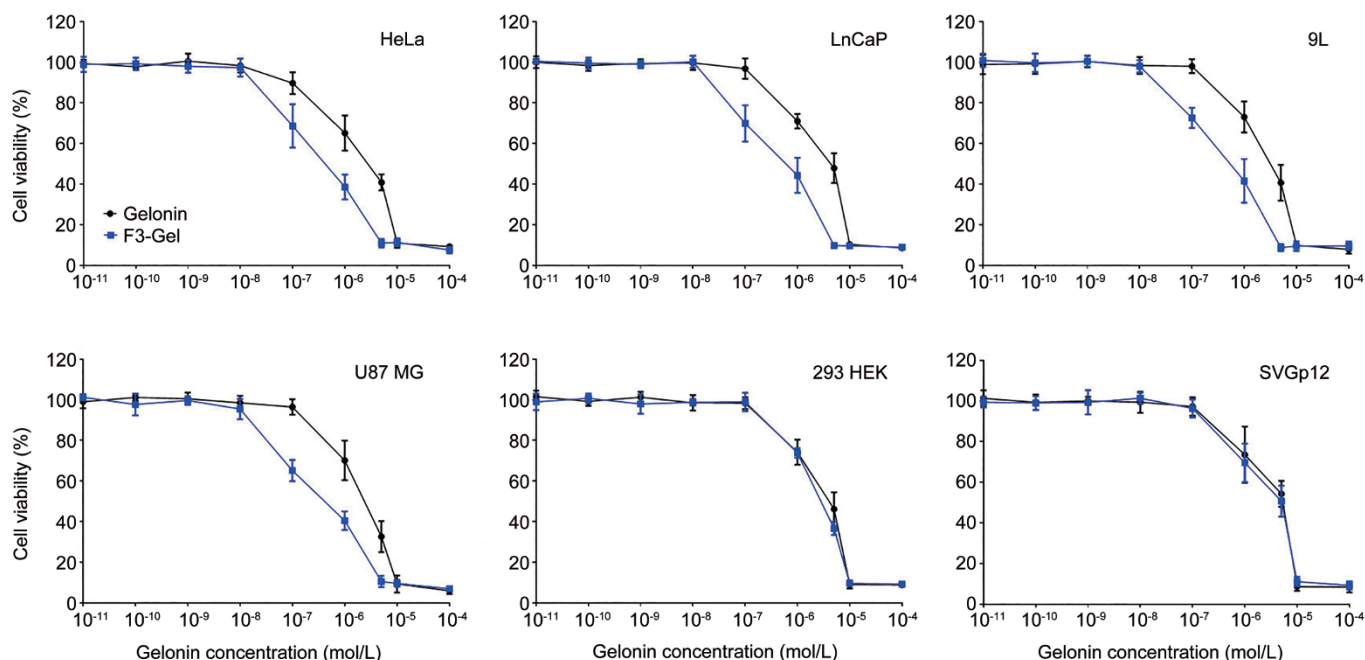


Figure 4. Cytotoxicity assay results. The viability profiles of cancer (HeLa, LnCaP, 9L and U87 MG) and noncancerous (293 HEK and SVGp12) cells were evaluated after 48 h of incubation with varied concentrations (10^{-11} – 10^{-4} $\mu\text{mol/L}$) of either gelonin or F3-Gel. Plots are depicted with the mean \pm SEM ($n=3$).

bated with F3-Gel. However, there was no significant difference in the cell viability between gelonin and F3-Gel against noncancerous cell lines (293 HEK and SVGp12).

Intracellular activity of F3-Gel for inhibition of protein translation

As shown in Figure 5, when the cellular activity of F3-Gel was evaluated in U87 MG cells, F3-Gel displayed significantly greater inhibition of protein translation than gelonin. While gelonin at concentrations up to 1 $\mu\text{mol/L}$ exerted no effect on the intracellular protein level, F3-Gel at 0.5 $\mu\text{mol/L}$ was able to reduce the protein level to less than 50%, suggesting internalization of only F3-Gel into the U87 MG cells at sub-micromolar concentrations.

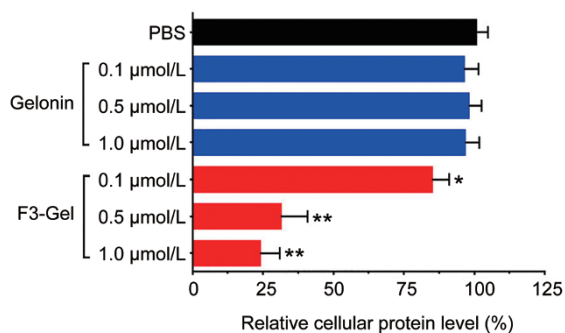


Figure 5. Intracellular activity of F3-Gel in U87 MG cells. Relative cellular protein levels in U87 MG cancer cells were measured after 24 h of incubation with gelonin or F3-Gel (at 0.1, 0.5 or 1 $\mu\text{mol/L}$). Control cells were incubated with PBS buffer. Plots are depicted with the mean \pm SEM ($n=3$).

Tissue distribution

The tissue distribution profiles of gelonin and F3-Gel were examined in U87 MG xenograft tumor-bearing mice. The fluorescence images of the major tissues harvested after administration of DylightTM 775-B4-labeled gelonin and F3-Gel at 1, 4 and 16 h post-administration are shown in Figures 6A and 6C, while the weight normalized MFIs (counts per gram tissue) of the organs are shown Figures 6B and 6D. As seen, basically, both gelonin and F3-Gel displayed similar distribution profiles, with both of them primarily observed in the kidney and liver along the time course, which are known as the major elimination organs. In addition, the heart MFI profiles indicated that both of the gelonin samples were rapidly eliminated (less than an hour). As shown in Figure 7, the major difference in the biodistribution profiles was the tumor residence time and the accumulation amount. While gelonin and F3-Gel were both clearly observed in the tumor, F3-Gel was observed at the tumor site for a longer period (up to 16 h post-administration). Moreover, F3-Gel showed significantly greater tumor accumulation (3.2-fold) than gelonin ($P=0.0064$ by unpaired *t*-test when the area under the curves of the tumors ($\text{AUC}_{\text{tumor}}$) were compared). The tumor-to-heart ratios were 1.2, 1.4 and 0.6 for gelonin at 1, 4 and 16 h post-administration, while they were 5.6, 3.9 and 1.9 for F3-Gel.

Tumor growth inhibition by F3-Gel

Preliminary *in vivo* studies were conducted to examine the efficacy of F3-Gel using a U87 MG sc xenograft tumor mouse model. The tumor growth profiles are shown in Figure 8A, and the body weight changes are shown in Figure 8B. As seen in Figure 8A, while PBS, gelonin and F3-Gel at low doses

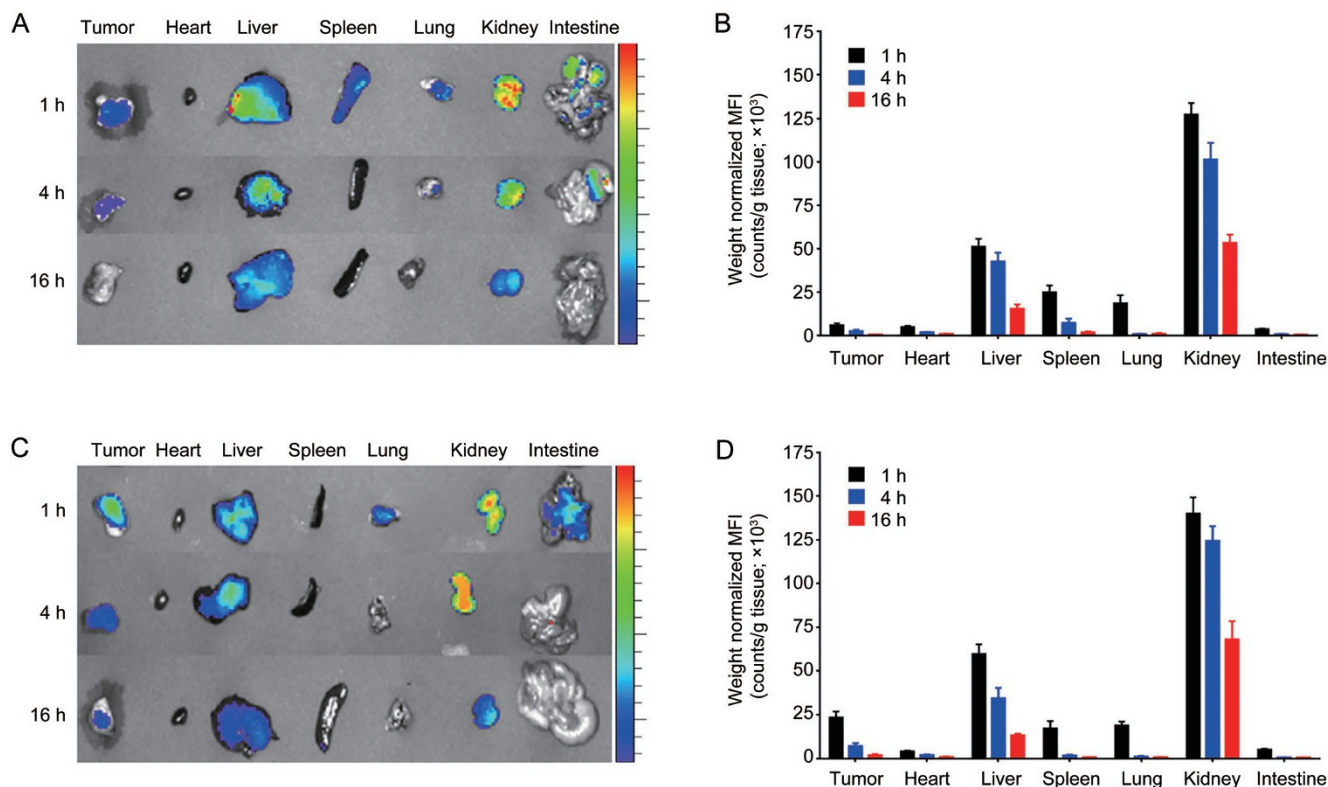


Figure 6. Organ distribution profiles of gelonin and F3-Gel in U87 MG sc xenograft tumor-bearing mice. (A) Biodistribution imaging of organs and (B) weight-normalized mean fluorescence intensity (MFI) values measured from each organ after administration with Dylight™ 775-B4-labeled gelonin. (C) Bioimaging results of organs and (D) weight-normalized MFI values after the administration of labeled F3-Gel via the tail vein. At the indicated time points (1, 4, and 16 h), major organs were harvested and imaged using an IVIS® spectrum imaging system equipped with an ICG filter (Ex/Em: 745/800 nm). Fluorescence intensities were observed in each organ up to 16 h, and MFI values were normalized by organ weights. Plots are depicted with the mean±SEM (n=6).

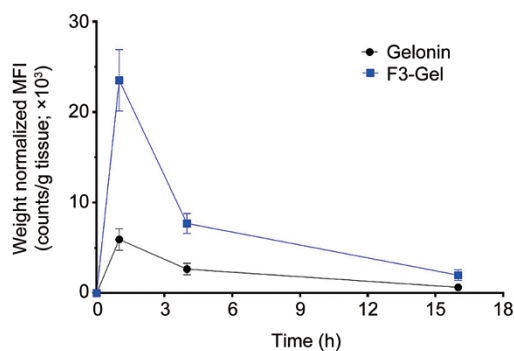


Figure 7. Tumor distribution profiles from the U87 MG xenograft mice until 16 h after administration with gelonin or F3-Gel. Weight-normalized mean fluorescence intensities in the tumor are displayed for both gelonin samples with the mean±SEM (n=6).

(0.125 and 0.25 μmol/kg) did not show any therapeutic effects, significant inhibition of the tumor growth was observed in the mice administered a high dose of F3-Gel (0.5 and 0.75 μmol/kg). Specifically, at d 25 (25 d after tumor implantation), compared with the PBS group (tumor size: 1110 mm³),

the average tumor size of mice treated with gelonin (1090 mm³) and low doses of F3-Gel (970 and 860 mm³ for 0.125 and 0.25 μmol/kg doses, respectively) exhibited non-significant effects on the tumor growth. However, in sharp contrast, high doses (0.5 and 0.75 μmol/kg) of F3-Gel exerted significant tumoricidal effects, with 36% (tumor size: 720 mm³) and 66% (380 mm³), respectively, inhibition of the tumor growth.

The average body weight changes of the mice during the efficacy study are shown in Figure 8B. As seen by d 25, the body weight of both the PBS control group and the 0.125 μmol/kg F3-Gel-treated mice continuously increased by an average of 23% and 22%, respectively. However, the mice treated with gelonin (0.75 μmol/kg dose) and higher doses of F3-Gel (0.25, 0.5 and 0.75 μmol/kg doses) experienced transient yet significant body weight loss. Specifically, by d 25, the body weight change of gelonin-treated mice was -14%, and the body weight changes of F3-Gel-treated mice (with 0.25, 0.5 and 0.75 μmol/kg dose) were 10%, -3% and -14%, respectively.

Discussion

Current chemotherapy for the treatment of cancer has posed challenges involving the ineffectiveness of anti-cancer small-molecule drugs as well as the dose-limiting toxicity caused by

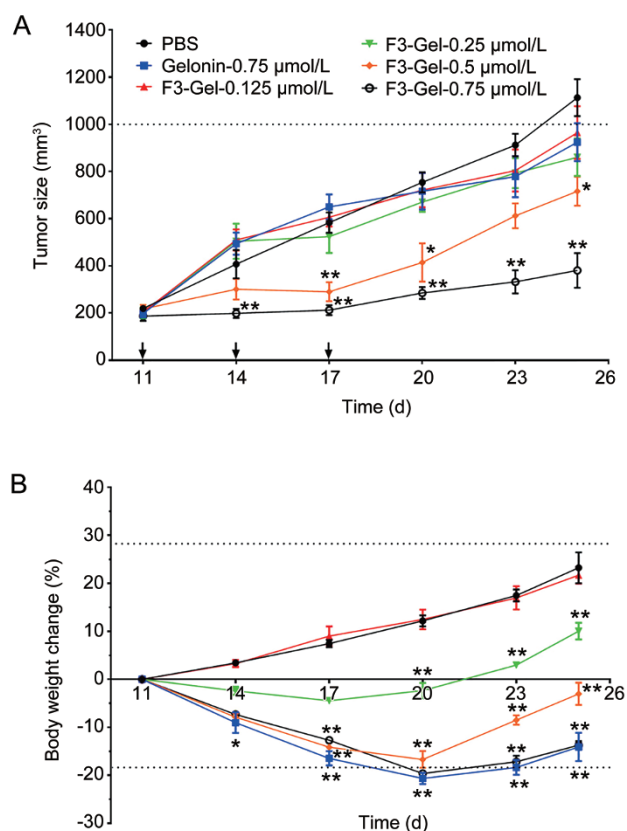


Figure 8. *In vivo* evaluation study of the therapeutic efficacy and toxicity of gelonin or F3-Gel in U87 MG xenograft tumor-bearing mice. U87 MG sc xenograft tumor-bearing mice were randomly divided into six groups when the tumor size reached an average of 200 mm³ (d 11 after administration). (A) Tumor volumes (mm³) and (B) body weight change (%) in mice at d 11, 14, 17, 20, 23, and 25 after tail vein injection of gelonin samples with either 1) PBS, 2) gelonin (0.75 µmol/kg), 3) F3-Gel (0.125 µmol/kg), 4) F3-Gel (0.25 µmol/kg), 5) F3-Gel (0.5 µmol/kg) or 6) F3-Gel (0.75 µmol/kg). The mice were treated a total of three times with the agents (1–6) at d 11, 14 and 17 via tail vein injection. The tumor volume and body weight of the mice were measured until the average tumor size of the PBS control group reached 1000 mm³. Mean±SEM (n=6). One-way ANOVA with Tukey's multiple comparison test as the *post hoc* test; **P*<0.05, ***P*<0.01.

the nonselective effects of such drugs on normal tissues. To overcome the therapeutic limitations of the existing small-molecule anti-cancer drugs, there has been rising interest in the use of highly potent macromolecular drugs and ligand-based delivery systems for selective tumor targeting. As potent toxins with N-glycosidase activity on 28S rRNA, several gelonin molecules are sufficient to kill a cell if they can enter the tumor cell and fully access the ribosomes inside the cell. However, gelonin by itself is not effective for cancer treatment because it does not have a cell binding-domain to mediate internalization into the cells^[20, 22]. Peptide ligands such as F3 peptide can facilitate the intracellular transport of cargoes by binding to nucleolins, cell surface receptors that are selectively expressed on tumor cell membranes^[17]. In this regard, in

this research, we have successfully engineered an F3-gelonin (F3-Gel) fusion chimera through a genetic recombination method without any significant influence on the intrinsic activities of gelonin or F3-peptide. This novel fusion toxin (F3-Gel) displayed significantly augmented cytotoxic activity against cancer cells compared with noncancerous cells, suggesting the feasibility of this selective therapeutic agent to overcome the current challenges in tumor targeting.

Regarding recombinant synthesis of F3-Gel chimera, we confirmed the expression and successful purification of F3-Gel from an *E coli* culture system as shown by the SDS-PAGE results (Figure 1C). The synthesis method of the fusion toxin is meaningful because when eukaryotic proteins are expressed by prokaryotic *E coli* cells, improper folding of proteins often occurs, producing insoluble aggregates called inclusion bodies. Referring to previous reports, the expression of proteins that are not easily produced in the *E coli* system can be improved by inclusion and co-expression of a highly expressible fusion partner^[27]. Based on this principle, we inserted the F3 peptide-Gelonin gene into a pET-TRX vector containing the thioredoxin (TRX) gene to create the pET-TRX-F3-Gel vector (Figure 1A). As a fusion partner, TRX is a small 12-kDa redox protein that can be overexpressed to a high level in *E coli* (accumulation of up to 40% of the cellular proteins) in a soluble form^[28]. The utility of TRX as a fusion partner for soluble expression of gelonin fusion proteins has already been reported in our previous publications^[24, 29]. Herein, we have clearly demonstrated the plausibility of this strategy, as the N-terminal thioredoxin-6×His tagged-gelonin-F3 peptide chimera (F3-Gel) was successfully produced in large quantities as a soluble protein in *E coli*.

Relevant studies regarding recombinant proteins have claimed that even a slight conformational change in the 3-D structure can result in a significant alteration in the biological activities of proteins^[30, 31]. Nevertheless, the data obtained using a cell-free translational system (a rabbit reticulocyte lysate assay) confirmed that the F3-Gel product possessed protein synthesis inhibition activity equivalent to that of unmodified gelonin (Figure 2). This result appears consistent with our previous reports that gelonin is quite stable in fusions due to its structure^[26, 32], which consequently contributes to the retention of its activity even after fusion with F3 peptide. To elucidate any anti-cancer targeting effects of F3-Gel or gelonin alone, for the *in vitro* cell experiments, we used HeLa, LnCaP, 9L, and U87 MG cancer cells because these cell lines were fully examined in other previous studies related to the F3 peptide^[18, 33]. In contrast to the equipotent intrinsic activity compared with unmodified gelonin in the cell-free conditions (Figure 2), in the U87 MG cell lines, F3-Gel exhibited a significantly greater ability to reduce the protein level to less than 50% than that of the gelonin (Figure 5). Moreover, when the cellular uptake in U87 MG cells was compared with that in the noncancerous 293 HEK cells after incubation with either TRITC-labeled gelonin or F3-Gel for up to 4 h, high F3-Gel fluorescence signals were exhibited in the U87 MG cells but not in the 293 HEK cells, while only low levels of gelonin

fluorescence were found in both cell types (Figure 3A). When the cell internalization profiles of gelonin and F3-Gel were compared for six different cell lines, significantly higher cellular uptake of F3-Gel was observed in all the tested cancer cells but not in the noncancerous cells (Table 1). Finally, these results support the notion that the F3 peptide in the F3-Gel fusion toxins might specifically bind to tumor-associated receptors exposed on the cell surface.

Because of the structural similarity, F3 peptide (KDEPQRRSARLSAKPAPPKPEPKPKKAPAKK; containing 3 arginine and 8 lysine residues) has often been compared with cationic cell penetrating peptides for any discriminative membrane penetration activity. However, similar to previous reports^[19, 34], our cellular study results with various cancer (eg, HeLa, LnCaP, 9L, and U87 MG) and noncancerous (293 HEK and SVGP12) cell lines clearly demonstrated the cancer targeting effects of F3 peptide (Figure 4 and Table 2). While significantly higher cytotoxicity was observed in the cancer cell lines incubated with F3-Gel than with gelonin, there was no significant difference in the cell viability between gelonin and F3-Gel against noncancerous cell lines, suggesting that intracellular uptake of F3-Gel into the tested cancer cells was mediated via specific binding of F3, presumably to the nucleolin exposed on the tumor cell surface. Nucleolin is known as a multifunctional DNA/RNA binding protein involved in regulation of gene transcription, chromatin remodeling, RNA metabolism, and ribosomal RNA synthesis^[19]. Tumor cells with high proliferation rates are known to overexpress surface-associated nucleolins in addition to cytoplasmic and nuclear nucleolins, whereas normal cells express nucleolins in the cytoplasm and nuclear membrane^[18]. Thus, surface nucleolins make tumor cells the preferential targets. Herein, the F3 peptide in the fused F3-Gel can interact with cell surface-associated nucleolins, a receptor shuttle, to efficiently internalize gelonin into the cytoplasm, resulting in protein synthesis inhibition and lower protein levels in the tumor cells.

U87 MG cells are known as human glioblastoma cell lines that overexpress nucleolins, localized in a phosphorylated and glycosylated form on the cell surface and nuclear membrane^[18]. As shown in Tables 1 and 2, the results of our *in vitro* cell experiment showed enhanced cellular uptake of F3-Gel and selective cytotoxicity in the U87 MG cells. Encouraged by the *in vitro* results, we established a tumor-bearing mouse model with U87 MG cell line xenografts to evaluate the feasibility of F3-Gel constructs for tumor targeting. Basically, in the *in vivo* distribution profiles in U87 MG xenograft tumor-bearing mice, both F3-Gel and unmodified gelonin showed similar biodistribution behaviors in normal tissues such as the kidney, liver, and heart (Figure 6). Remarkably, F3-Gel was accumulated at 3.2-fold higher levels in the tumor site for a prolonged time (up to 16 h post-administration) compared with gelonin (Figure 7). Specifically, the tumor-to-heart ratio of F3-Gel (higher than 1.0) supports efficient tumor targeting, presumably via interaction between F3 peptide and the nucleolin receptor.

In vivo efficacy studies showed that a high dose of F3-Gel

exerted significant anti-tumor activity (Figure 8A). However, body weight loss, a typical sign of transient but severe toxicity, was accompanied with the high dose of F3-Gel (Figure 8B). Both gelonin and F3-Gel were shown to cause severe body weight loss at 0.75 $\mu\text{mol}/\text{kg}$. This could be presumably explained by renal toxicity caused by rapid accumulation of the gelonin samples in the kidney. At the medium dose of F3-Gel, anti-tumor effects were still significant but were associated with less body weight loss compared with gelonin alone, evidencing the feasibility of the F3 peptide fusion strategy. Meanwhile, when the mean fluorescence intensity (MFI) values in the heart tissues were compared (Figure 6), both F3-Gel and unmodified gelonin displayed rapid distribution and elimination profiles, presumably due to their sizes. Since both gelonin samples are smaller than albumin (66.7 kDa) and the plasma half-life of gelonin is only 3 min (data not shown), gelonin and F3-Gel might be eliminated from the body primarily by renal excretion with a shorter systemic circulation. To overcome the issues related to the short half-life and intrinsic toxicity at high doses of F3-Gel, further studies are underway to develop a nanoparticle-based drug delivery system to extend the plasma half-life and increase the tumor targeting efficiency at the lower dose. Based on reports that the interaction between nucleolin-targeted ligands and nucleolin is influenced by the isoelectric point^[33, 35], it would be helpful to devise appropriate delivery vehicles for the F3-Gel by optimizing the physicochemical properties, such as surface charge, in the presence of F3 peptide to enable an efficient and safe therapeutic effect of F3-Gel.

Conclusion

In this research, we evaluated the applicability of novel recombinant gelonin with F3 peptide for anti-cancer efficacy *in vitro* and *in vivo*. This is the first attempt to synthesize gelonin fused with F3 peptide using a recombinant DNA method, and the fused plasmid vector was successfully produced from *E. coli*. Based on the microscopic results and cytotoxicity tests, F3 peptide might contribute to transferring gelonin into cell nuclei, enhancing apoptotic effects. An *in vivo* study with a cancer cell xenograft mouse model confirmed that administration of F3-Gel could exert significant anti-tumor efficacy when compared with the administration of gelonin alone. Overall, this research demonstrated an effective yet safe method for delivering highly potent toxins such as gelonin to tumor sites by utilizing F3 peptide, a so-called helper peptide.

Acknowledgements

This work was financially supported by grants from the Basic Science Research Program through the National Research Foundation of Korea (NRF), funded by the Ministry of Education, Science and Technology (NRF-2015R1C1A1A02036781 to Meong Cheol SHIN and NRF-2015R1A6A3A01020598 to Kyoung Ah MIN). Additionally, this work (2015-04-017) was partly supported by the Fund for New Professor Research Foundation Program, Gyeongsang National University, 2015. We thank Dr Wolfgang E TROMMER (University of Kaiser-

slautern, Germany) for the gelonin expression vector (pET28a-Gel).

References

- 1 Rabik CA, Dolan ME. Molecular mechanisms of resistance and toxicity associated with platinating agents. *Cancer Treat Rev* 2007; 33: 9–23.
- 2 Giacchetti S, Itzhaki M, Gruia G, Adam R, Zidani R, Kunstlinger F, *et al*. Long-term survival of patients with unresectable colorectal cancer liver metastases following infusional chemotherapy with 5-fluorouracil, leucovorin, oxaliplatin and surgery. *Ann Oncol* 1999; 10: 663–9.
- 3 Imai K, Takaoka A. Comparing antibody and small-molecule therapies for cancer. *Nat Rev Cancer* 2006; 6: 714–27.
- 4 Allen TM. Ligand-targeted therapeutics in anticancer therapy. *Nat Rev Cancer* 2002; 2: 750–63.
- 5 Hu Q, Gu G, Liu Z, Jiang M, Kang T, Miao D, *et al*. F3 peptide-functionalized PEG-PLA nanoparticles co-administrated with tLyp-1 peptide for anti-glioma drug delivery. *Biomaterials* 2013; 34: 1135–45.
- 6 Sinha R, Kim GJ, Nie S, Shin DM. Nanotechnology in cancer therapeutics: bioconjugated nanoparticles for drug delivery. *Mol Cancer Ther* 2006; 5: 1909–17.
- 7 Weiner LM, Surana R, Wang S. Monoclonal antibodies: versatile platforms for cancer immunotherapy. *Nat Rev Immunol* 2010; 10: 317–27.
- 8 Lewis Phillips GD, Li G, Dugger DL, Crocker LM, Parsons KL, Mai E, *et al*. Targeting HER2-positive breast cancer with trastuzumab-DM1, an antibody-cytotoxic drug conjugate. *Cancer Res* 2008; 68: 9280–90.
- 9 Alley SC, Okeley NM, Senter PD. Antibody-drug conjugates: targeted drug delivery for cancer. *Curr Opin Chem Biol* 2010; 14: 529–37.
- 10 Scott AM, Wolchok JD, Old LJ. Antibody therapy of cancer. *Nat Rev Cancer* 2012; 12: 278–87.
- 11 Harding FA, Stickler MM, Razo J, DuBridge RB. The immunogenicity of humanized and fully human antibodies: residual immunogenicity resides in the CDR regions. *MAbs* 2010; 2: 256–65.
- 12 Rudnick SI, Lou J, Shaller CC, Tang Y, Klein-Szanto AJ, Weiner LM, *et al*. Influence of affinity and antigen internalization on the uptake and penetration of Anti-HER2 antibodies in solid tumors. *Cancer Res* 2011; 71: 2250–9.
- 13 Barry MA, Dower WJ, Johnston SA. Toward cell-targeting gene therapy vectors: selection of cell-binding peptides from random peptide-presenting phage libraries. *Nat Med* 1996; 2: 299–305.
- 14 Lu Y, Low PS. Folate-mediated delivery of macromolecular anticancer therapeutic agents. *Adv Drug Deliv Rev* 2002; 54: 675–93.
- 15 Wang AZ, Gu F, Zhang L, Chan JM, Radovic-Moreno A, Shaikh MR, *et al*. Biofunctionalized targeted nanoparticles for therapeutic applications. *Expert Opin Biol Ther* 2008; 8: 1063–70.
- 16 Makela AR, Matilainen H, White DJ, Ruoslahti E, Oker-Blom C. Enhanced baculovirus-mediated transduction of human cancer cells by tumor-homing peptides. *J Virol* 2006; 80: 6603–11.
- 17 Qin M, Zong H, Kopelman R. Click conjugation of peptide to hydrogel nanoparticles for tumor-targeted drug delivery. *Biomacromolecules* 2014; 15: 3728–34.
- 18 Destouches D, El Khoury D, Hamma-Kourbali Y, Krust B, Albanese P, Katsoris P, *et al*. Suppression of tumor growth and angiogenesis by a specific antagonist of the cell-surface expressed nucleolin. *PLoS One* 2008; 3: e2518.
- 19 Christian S, Pilch J, Akerman ME, Porkka K, Laakkonen P, Ruoslahti E. Nucleolin expressed at the cell surface is a marker of endothelial cells in angiogenic blood vessels. *J Cell Biol* 2003; 163: 871–8.
- 20 Puri M, Kaur I, Perugini MA, Gupta RC. Ribosome-inactivating proteins: current status and biomedical applications. *Drug Discov Today* 2012; 17: 774–83.
- 21 Kay MA. State-of-the-art gene-based therapies: the road ahead. *Nat Rev Genet* 2011; 12: 316–28.
- 22 Min KA, He H, Yang VC, Shin MC. Construction and characterization of gelonin and saporin plasmids for toxic gene-based cancer therapy. *Arch Pharmacol Res* 2016; 39: 677–86.
- 23 Atkinson SF, Bettinger T, Seymour LW, Behr JP, Ward CM. Conjugation of folate via gelonin carbohydrate residues retains ribosomal-inactivating properties of the toxin and permits targeting to folate receptor positive cells. *J Biol Chem* 2001; 276: 27930–5.
- 24 Shin MC, Zhao J, Zhang J, Huang Y, He H, Wang M, *et al*. Recombinant TAT-gelonin fusion toxin: synthesis and characterization of heparin/protamine-regulated cell transduction. *J Biomed Mater Res Part A* 2015; 103: 409–19.
- 25 Shin MC, Zhang J, Min KA, He H, David AE, Huang Y, *et al*. PTD-modified ATTEMPTS for enhanced toxin-based cancer therapy: an *in vivo* proof-of-concept study. *Pharm Res* 2015; 32: 2690–703.
- 26 Shin MC, Min KA, Cheong H, Moon C, Huang Y, He H, *et al*. Preparation and characterization of gelonin-melittin fusion biotoxin for synergistically enhanced anti-tumor activity. *Pharm Res* 2016; 33: 2218–28.
- 27 LaVallie ER, DiBlasio-Smith EA, Collins-Racie LA, Lu Z, McCoy JM. Thioredoxin and related proteins as multifunctional fusion tags for soluble expression in *E coli*. *Methods Mol Biol* 2003; 205: 119–40.
- 28 Singh SM, Panda AK. Solubilization and refolding of bacterial inclusion body proteins. *J Biosci Bioeng* 2005; 99: 303–10.
- 29 Shin MC, Zhang J, Min KA, Lee K, Moon C, Balthasar JP, *et al*. Combination of antibody targeting and PTD-mediated intracellular toxin delivery for colorectal cancer therapy. *J Control Rel* 2014; 194: 197–210.
- 30 Battelli MG, Barbieri L, Stirpe F. Toxicity of, and histological lesions caused by, ribosome-inactivating proteins, their IgG-conjugates, and their homopolymers. *APMIS* 1990; 98: 585–93.
- 31 Ebert RF, Spryn LA. Immunotoxin construction with a ribosome-inactivating protein from barley. *Bioconjug Chem* 1990; 1: 331–6.
- 32 Hosur MV, Nair B, Satyamurthy P, Misquith S, Suroliya A, Kannan KK. X-ray structure of gelonin at 1.8 Å resolution. *J Mol Biol* 1995; 250: 368–80.
- 33 Hovanessian AG, Soundaramourty C, El Khoury D, Nondier I, Svab J, Krust B. Surface expressed nucleolin is constantly induced in tumor cells to mediate calcium-dependent ligand internalization. *PLoS One* 2010; 5: e15787.
- 34 Porkka K, Laakkonen P, Hoffman JA, Bernasconi M, Ruoslahti E. A fragment of the HMGN2 protein homes to the nuclei of tumor cells and tumor endothelial cells *in vivo*. *Proc Natl Acad Sci U S A* 2002; 99: 7444–9.
- 35 Zhang Y, Yang M, Park JH, Singelyn J, Ma H, Sailor MJ, *et al*. A surface-charge study on cellular-uptake behavior of F3-peptide-conjugated iron oxide nanoparticles. *Small* 2009; 5: 1990–6.